### 1 DoubletFinder: Doublet detection in single-cell RNA sequencing data using artificial 2 nearest neighbors

- 3 Christopher S. McGinnis<sup>1</sup>, Lyndsay M. Murrow<sup>1</sup> and Zev J. Gartner<sup>1,2,3,4</sup>\*
- <sup>1</sup>Department of Pharmaceutical Chemistry, University of California, San Francisco
- 5 <sup>2</sup>Chan Zuckerbeg Biohub, University of California, San Francisco
- 6 <sup>3</sup>Center for Cellular Construction, University of California, San Francisco, San Francisco, CA 94158, USA
- 7 <sup>4</sup>Lead Contact
- 8 \*Correspondence: <u>zev.gartner@ucsf.edu</u> 9
- 10 SUMMARY

11 Single-cell RNA sequencing (scRNA-seq) using droplet microfluidics occasionally 12 produces transcriptome data representing more than one cell. These technical artifacts are caused by cell doublets formed during cell capture and occur at a frequency proportional to the 13 14 total number of sequenced cells. The presence of doublets can lead to spurious biological 15 conclusions, which justifies the practice of sequencing fewer cells to limit doublet formation rates. Here, we present a computational doublet detection tool – DoubletFinder – that identifies 16 17 doublets based solely on gene expression features. DoubletFinder infers the putative gene expression profile of real doublets by generating artificial doublets from existing scRNA-seg data. 18 19 Neighborhood detection in gene expression space then identifies sequenced cells with 20 increased probability of being doublets based on their proximity to artificial doublets. 21 DoubletFinder robustly identifies doublets across scRNA-seq datasets with variable numbers of 22 cells and sequencing depth, and predicts false-negative and false-positive doublets defined 23 using conventional barcoding approaches. We anticipate that DoubletFinder will aid in scRNA-24 seg data analysis and will increase the throughput and accuracy of scRNA-seg experiments.

25

## 26 INTRODUCTION

27 Since its introduction nearly a decade ago, scRNA-seq has been used to elucidate 28 previously unknown cell types and reconstruct developmental dynamics among heterogeneous 29 cell populations (Human Cell Atlas Consortium, 2017). At first, scRNA-seq workflows were

limited to tens to hundreds of cells which hindered data interpretation due to batch effects and 30 31 low statistical power (Stegle et al., 2016). Today, sequencing thousands to hundreds of 32 thousands of cells is routine due to the advent of droplet microfluidics and nanowell-based sequencing strategies (Macosko et al., 2015; Klein et al., 2015; Zheng et al., 2017; Gierahn et 33 al., 2017; Takara Bio USA, 2018). These techniques rely on a Poisson loading strategy to 34 35 compartmentalize individual cells and mRNA capture beads before cell lysis, mRNA capture, 36 and transcript barcoding via reverse transcription. Since cells are captured randomly, the proportion of droplets containing >1 cell - known as doublets - scales linearly across an 37 38 experimentally-relevant range of input cell concentrations (10X Genomics, 2017), justifying the 39 practice of limiting the number of sequenced cells to minimize doublet formation rates.

The confounding effects of doublets in scRNA-seq data are well-appreciated (llicic et al., 40 41 2016). However, genomic and cellular barcoding techniques for identifying doublets have only 42 recently been developed (Stoeckius et al., 2017; Kang et al., 2018; Gehring et al., 2018; Guo et 43 al., 2018; Rosenberg et al., 2018). In one such strategy, distinct samples receive unique oligonucleotide barcodes delivered by conjugation to antibodies targeting broadly expressed 44 45 cell-surface antigens. When the barcoded pools are combined and sequenced, doublets can be identified according to the co-occurrence of orthogonal cell 'hashtags' (Stoeckius et al., 2017). 46 47 In a second strategy, doublets in a pooled population of cells from different individuals are identified by a computational pipeline. Demuxlet, which facilitates doublet inference based on 48 49 the co-occurrence of mutually-exclusive SNP profiles (Kang et al., 2018).

50 By detecting doublets, both Demuxlet and Cell Hashing minimize technical artifacts while 51 enabling users to "superload" droplet microfluidics devices for increased scRNA-seq throughput. 52 However, both methods have limitations. First, neither method can identify doublets formed from 53 identically-barcoded cells. Second, neither method is universally applicable across experimental systems, since Demuxlet requires genetically distinct samples and Cell Hashing requires unique antibody-oligonucleotide conjugate panels for the cell types and species of interest. Third, neither method can be used to analyze existing scRNA-seq datasets. For these reasons, computational methods for defining doublets based on gene expression patterns alone are highly desirable.

59 Here, we present DoubletFinder, a computational doublet detection tool that relies solely on gene expression data. Beginning with the observation that doublets cluster separately from 60 61 singlets in high-dimensional gene expression space (Stoeckius et al., 2017; Kang et al., 2018), 62 we reasoned that real doublets would cluster together with synthetic doublets formed by 63 averaging the expression data of two real cells. By merging artificial doublets with existing 64 scRNA-seq data, we can distinguish doublets from singlets according to the proportion of 65 artificial nearest neighbors (pANN) for each real cell in gene expression space. Thresholding the 66 resulting pANN distribution to match the expected number of doublets provides an accurate 67 metric for doublet prediction that can be applied to any scRNA-seq dataset.

68

#### 69 RESULTS

70 DoubletFinder predicts doublets more accurately than nUMIs: Existing strategies for identifying 71 doublets using gene expression features primarily rely on two sources of information. First, since 72 the total number of captured mRNA molecules is expected to be greater for doublets than 73 singlets, doublets are commonly excluded by thresholding cells with high numbers of unique 74 molecular identifiers (nUMIs; Islam et al., 2014; Ziegenhain et al., 2017). While intuitively appealing, technical variability in mRNA capture efficiency and biological variability in mRNA 75 76 content limits the utility of nUMI-based doublet predictions (Stoeckius et al., 2017). In a second 77 strategy, doublets are removed from scRNA-seq data by identifying groups of cells exhibiting

the co-expression of genes with non-overlapping expression patterns *in vivo* (Rosenberg et al., 2018). This strategy cannot be applied to biological systems where such marker genes are unknown, undetected, or unavailable. Moreover, such a strategy could theoretically lead to the erroneous removal of new cell types or developmental states with intermediate expression profiles (Fig. 1A). Given these shortcomings, new methods for predicting doublets using gene expression features alone would greatly benefit the single-cell genomics field.

84 DoubletFinder predicts doublets in a fashion agnostic to nUMIs, marker gene expression, 85 genetic background or exogenous barcodes and can be split into four distinct steps: (1) Generate 86 artificial doublets. (2) Merge real and artificial data and reduce dimensionality with principal 87 component analysis (PCA), (3) Define the nearest neighbors for every real cell in PC space, and 88 (4) Compute and threshold the proportion of artificial nearest neighbors (pANN; Fig. 1B). We 89 tested the efficacy of DoubletFinder against scRNA-seq datasets where doublets are empiricallydefined: The publically-available Cell Hashing and Demuxlet datasets comprised of 15,178 and 90 91 35,524 peripheral blood mononuclear cells (PBMCs), respectively. Demuxlet PBMCs were 92 derived from 8 genetically-distinct human sources while Cell Hashing PBMCs were barcoded 93 with 8 distinct antibody-oligonucleotide conjugate panels. Using optimized input parameters 94 (Supplementary Materials, Fig. S1), we tested whether pANN outperforms nUMIs as a doublet-95 prediction feature by using receiver operating curve (ROC) analysis to compare logistic 96 regression models trained on the Cell Hashing data using pANN alone, nUMIs alone, or both 97 (Fig. 1C). ROC analysis demonstrates that pANN predicts doublets more accurately than nUMIs. 98 Moreover, the model trained with both features performed nearly indistinguishably to the pANN-99 alone model, suggesting that DoubletFinder captures all of the doublet-specific information 100 inherent to nUMIs.

102 DoubletFinder predicts Cell Hashing doublets: To make specific doublet predictions for each 103 cell, DoubletFinder rank-orders cells by their pANN values and thresholds this list according to 104 the number of expected doublets. To test the robustness of pANN thresholding, the number of 105 expected doublets was determined using two different strategies (Fig. 1D). First, since 8 samples 106 were multiplexed in the Cell Hashing and Demuxlet studies, we reasoned that 1/8 of the true 107 doublets were undetected because they were formed from genetically-identical or identically-108 barcoded cells. Thus, we thresholded pANN according to the number of detected doublets with 109 an assumed 12.5% false negative rate ( $\beta$ ). Second, since the doublet formation rate can be 110 accurately estimated by applying Poisson statistics to the number of cells loaded into the droplet 111 microfluidics device (10X Genomics, 2017), we thresholded pANN according to this rate. For 112 standard scRNA-seq experiments where doublets are not empirically-defined, pANN can only 113 be thresholded using the Poisson strategy.

Depending on the threshold used, DoubletFinder predicted 2680 or 2155 doublets when 114 115 applied to the full Cell Hashing dataset. Single-cell gene expression data was visualized using 116 t-stochastic neighborhood embedding (t-SNE; van der Maaten and Hinton, 2008) and cells were 117 colored according to their real and predicted doublet status (Fig. 1E). Visual comparison of 118 doublets in t-SNE space illustrates that DoubletFinder predictions closely track Cell Hashing 119 results. This result is further supported by the observation that the frequency of DoubletFinder 120 predictions is highly enriched in Cell Hashing-defined doublet groups relative to singlet groups 121 (Fig. 1F), regardless of the thresholding strategy used.

122

<u>DoubletFinder predicts Cell Hashing false-negatives</u>: DoubletFinder predictions exhibit a less
 'speckled' appearance in t-SNE space relative to the Cell Hashing results (Fig. 2A, insets).
 Considering that doublets often cluster separately from singlets in gene expression space

126 (Stoeckius et al., 2017; Kang et al., 2018), we reasoned that cells called as singlets via Cell 127 Hashing, that nonetheless co-cluster with high-confidence doublets, are actually false-negatives 128 derived from identically-barcoded cells. Two main predictions follow from this line of reasoning. 129 First, if the putative false negatives are truly doublets, then they should exhibit gene expression 130 patterns associated with distinct cell types. In line with this prediction, Cell Hashing-defined 131 doublets and singlets in the highlighted region express marker genes for both B cells and NK 132 cells (Fig. 2B) – hematopoietic cell types that do not share a common progenitor in peripheral blood. Second, since false negative cells would be associated with the combined barcodes of 133 134 two cells, the nUMI counts for the most abundant barcode should be significantly higher in false negatives than high-confidence doublets. Moreover, since false negatives would not be 135 136 associated with high levels of multiple barcodes, the second most abundant barcode should be 137 similar to high-confidence singlets and significantly lower relative to high-confidence doublets. Statistical analysis supports these predictions (Wilcoxon rank sum test,  $p < 10^{-13}$ ; Fig. 2C). 138 139 Collectively, these results demonstrate that DoubletFinder robustly recapitulates doublet 140 assignments and accurately predicts Cell Hashing false-negatives.

141

DoubletFinder predicts Demuxlet doublets and identifies putative false-positives: To test whether DoubletFinder performance is sensitive to changes in the number of sequenced cells and sequencing depth, we applied DoubletFinder to the Demuxlet dataset. In addition to having more cells than the Cell Hashing data, the average number of UMIs (2408 vs 676) and genes (837 vs 376) per cell is also greater in the Demuxlet data. In line with our previous results, visual comparison of real and predicted doublets using t-SNE illustrates that DoubletFinder successfully identifies all doublet-enriched regions in gene expression space (Fig. 2D).

149 As with our Cell Hashing comparison, there were a number of regions in gene expression 150 space where DoubletFinder predictions differed from Demuxlet classifications. Specifically, there 151 were many DoubletFinder-defined doublets called as singlets by Demuxlet that give doublet-152 enriched clusters the 'speckled' appearance discussed above. Moreover, in contrast to the Cell 153 Hashing comparison, there was a subset of cells classified as doublets by Demuxlet and singlets 154 using DoubletFinder (Fig. 2D, insets). Interestingly, the majority of these discordant calls are 155 scattered amongst high-confidence singlet clusters in gene expression space. This observation 156 can be explained by two alterative models. In one model, these discordant calls are caused by 157 homotypic doublets – i.e., doublets formed from cells of the same type – which presumably have 158 a similar transcriptional profile to singlets and, thus, would be more difficult for DoubletFinder to 159 detect relative to heterotypic doublets. Alternatively, the discordant calls are due to false-positive 160 Demuxlet classifications.

If these cells were in fact homotypic doublets left undetected by DoubletFinder, then one 161 162 would expect that DoubletFinder was insensitive to homotypic doublets throughout the Demuxlet 163 dataset. To test this possibility, we tracked the cell types comprising each artificial doublet and 164 deconvolved pANN values into homotypic and heterotypic components. Visualization of cells 165 with majority homotypic or heterotypic nearest neighbors highlights a region of homotypic 166 doublets formed from CD4<sup>+</sup> T-cells (Fig. 2E; Supplementary Materials, Fig. S2), which suggests 167 that DoubletFinder has the sensitivity to detected certain classes of homotypic doublets. 168 Moreover, the scattering of discordant doublet classifications amongst high-confidence singlet 169 clusters in gene expression space is also evident in Demuxlet classifications of the Cell Hashing 170 data (Supplementary Materials, Fig. S2). Cell Hashing is sensitive to homotypic doublets, which suggests that the discordant calls are not a consequence of homotypic doublets missed by 171 172 DoubletFinder. Finally, if the putative false-positive calls are homotypic doublets, one would

expect the number of RNA UMIs to approximate levels observed for high-confidence doublets. Interestingly, the RNA nUMI distribution for putative false-positives is nearly indistinguishable to high-confidence singlets (Wilcoxon rank sum test, p = 0.34), while high-confidence doublets and putative false-negatives are both significantly enriched for RNA nUMIs (Wilcoxon rank sum test,  $p < 10^{-15}$ ; Fig. 2F). While it is difficult to definitively ascertain the ground truth for these discordant calls, these results collectively demonstrate that DoubletFinder is robust across a range of cell numbers and sequencing depths and prospectively predicts Demuxlet false-positives.

180

#### 181 **DISCUSSION**

182 High-throughput scRNA-seg suffers from the formation of doublets due to the inherent 183 nature of Poisson cell loading. Doublets can lead to spurious conclusions during analysis when 184 left unidentified because the resulting artefactual expression data may be interpreted as previously-undescribed cell types, developmental intermediates, or disease states. As a result, 185 186 it has become common practice to minimize the doublet formation rate by minimizing the ratio 187 of sequenced cells to mRNA capture beads. Although recent advances in direct doublet 188 detection methodologies have proven to be effective, they are not universally or retroactively 189 applicable. For this reason, complementary techniques for predicting doublets based only on 190 gene expression data have the potential to further increase scRNA-seg throughput while removing technical artifacts. 191

Towards this goal, DoubletFinder accurately identifies doublets in scRNA-seq data by integrating artificial doublets into real data and computing the pANN for every real cell. We have shown that DoubletFinder distinguishes real doublets from singlets better than nUMIs in the Cell Hashing dataset. Moreover, we demonstrate that DoubletFinder accurately predicts doublets for two independent PBMC scRNA-seq datasets of different sizes and sequencing depths. As these

are the only publically available data with empirically-defined doublets, it is unclear whether 197 198 DoubletFinder will require further optimization for scRNA-seq datasets describing different 199 tissues or biological systems. We have also shown that DoubletFinder identifies false-negative 200 and putative false-positive doublet classifications present in these datasets, which supports the 201 use of DoubletFinder in concert with Cell Hashing, Demuxlet, and other barcoding approaches. 202 Finally, we demonstrate that DoubletFinder performs robustly with pANN thresholding strategies 203 that differed by >5000 cells (Fig. 1D). This suggests that DoubletFinder can be applied in 204 experimental contexts where doublet formation rates differ significantly from industry estimates 205 - e.g., clumpy single-cell suspensions or especially cohesive cell types. Collectively, 206 DoubletFinder represents a fast, easy-to-use doublet detection strategy that will aid the single-207 cell genomics community in data analysis and enable high-throughput scRNA-seq technologies 208 to be utilized to their fullest potential.

209

#### 210 MATERIALS & METHODS

211 <u>DoubletFinder Overview</u>: Artificial doublets were generated from raw UMI count matrices via 212 random sampling of cell expression profiles without replacement before pre-processing using 213 the 'Seurat' R package, as described previously (Butler et al., 2018). Notably, no sources of 214 variation were regressed out of the merged data before PCA, and the top 10 PCs – chosen via 215 inflection point estimation on the corresponding elbow plot – were used to define the Euclidean 216 distance matrix using the 'dist' R function.

217

218 <u>ROC Analysis</u>: ROC analysis-based model comparisons were performed using the 'ROCR' 219 (Sing et al., 2005) and 'pROC' (Robin et al., 2011) R packages. Briefly, logistic regression 220 models were defined on a training set comprising half the total data using the 'glm' R function

221	with the link argument set to 'logit'. These models were then used to create a vector describing
222	each cell's doublet probability with the 'predict' R function. ROC analysis was then performed by
223	calculating the sensitivity and specificity of doublet predictions based on the aforementioned
224	probability vector at varying probability thresholds. The AUC was then calculated for the resulting
225	curve, and AUC was used as a proxy for doublet detection model performance.
226	
227	Statistical Analysis: Statistically-significant differences between UMI levels were defined using
228	the Wilcoxon rank sum test implemented with the 'pairwisewilcox.test' R function. Multiple
229	comparison correction was performed using the Benjamini-Hochberg procedure.
230	
231	Data Availability: Cell Hashing (GEO: GSE108313) and Demuxlet (GEO: GSE96583) UMI count
232	matrices were downloaded from the Gene Expression Omnibus. DoubletFinder is implemented
233	as a fast, easy-to-use R package that interfaces with Seurat version 2.0 and higher.
234	DoubletFinder can be downloaded from GitHub (github.com/chris-mcginnis-ucsf/DoubletFinder).
235	
236	ACKNOWLEDGMENTS
237	We thank Matt Thomson (California Institute of Technology) for helpful discussion, as well as
238	Jimmie Ye (UCSF), Marlon Stoeckius and Shiwei Zheng (New York Genome Center) for
239	providing data access.
240	
241	AUTHOR CONTRIBUTIONS

C.S.M., L.M.M., and Z.J.G conceptualized the method and wrote the manuscript. C.S.M. wrotethe software and performed all bioinformatics analyses.

bioRxiv preprint doi: https://doi.org/10.1101/352484; this version posted July 19, 2018. The copyright holder for this preprint (which was not certified by peer review) is the author/funder. All rights reserved. No reuse allowed without permission.

# 245 DECLARATION OF INTERESTS

- 246 The authors declare no conflict of interest.
- 247
- 248 FUNDING
- 249 This research was supported in part by grants from the Department of Defense Breast Cancer
- 250 Research Program (W81XWH-10-1-1023 and W81XWH-13-1-0221), the NIH Common Fund
- (DP2 HD080351-01), the NSF (MCB-1330864), and the UCSF Center for Cellular Construction
- (DBI-1548297), an NSF Science and Technology Center. Z.J.G is a Chan-Zuckerberg Biohub
- 253 Investigator. L.M.M is a Damon Runyon Fellow supported by the Damon Runyon Cancer
- 254 Research Foundation (DRG-2239-15).

#### 255 256 **REFERENCES**

257 258

259 260

261

265

266

- 1. The HCA Consortium. The Human Cell Atlas White Paper. 2017. Retrieved from: humancellatlas.org/files/HCA\_WhitePaper\_18Oct2017.pdf
- 2. Stegle O, Teichmann SA, Marioni JC. Computational and analytical challenges in singlecell transcriptomics. Nat Rev Genet. 2015; 16(3):133-45.
- Macosko EZ, Basu A, Satija R, Nemesh J, Shekhar K, Goldman M, et al. Highly Parallel
  Genome-wide Expression Profiling of Individual Cells Using Nanoliter Droplets. 2015.
  Cell; 161(5):1202-1214.
  - Klein AM, Mazutis L, Akartuna I, Tallapragada N, Veres A, Li V, et al. Droplet barcoding for single-cell transcriptomics applied to embryonic stem cells. 2015. Cell; 161(5):1187-1201.
- Zheng GX, Terry JM, Belgrader P, Ryvkin P, Bent ZW, Wilson R, et al. Massively parallel
  digital transcriptional profiling of single cells. Nat Commun. 2017; 8:14049.
- Gierahn TM, Wadsworth MH 2nd, Hughes TK, Bryson BD, Butler A, Satija R, *et al.* Seq Well: portable, low-cost RNA sequencing of single cells at high throughput. Nat Methods.
  2017; 14(4):395-398.
- 7. Takara Bio USA. Full-length, single-cell RNA-seq with the SMARTer<sup>™</sup> ICELL8<sup>®</sup> Single-Cell System (Application note 633878). Mountain View, CA: Takara Bio. 2018. Available from:
- 276 clontech.com/US/Products/cDNA\_Synthesis\_and\_Library\_Construction/NGS\_Automati
  277 on/Single-Cell\_Automation/Single-Cell\_Automation\_Overview?sitex=10020:22372:US
- 10X Genomics. ChromiumTM Single Cell 3' Reagent Kits v2 User Guide. Pleasanton,
  CA: 10X Genomics. 2017.

- 9. Ilicic T, Kim JK, Kolodziejczyk AA, Bagger FO, McCarthy DJ, Marioni JC, Teichmann SA.
  Classification of low quality cells from single-cell RNA-seq data. Genome Biol. 2016
  17:29.
- 10. Stoeckius M, Zheng S, Houck-Loomis B, Hao S, Yeung BZ, Smibert P, Satija R. Cell
  "hashing" with barcoded antibodies enables multiplexing and doublet detection for single
  cell genomics. 2017. Preprint. bioRxiv doi: 10.1101/237693.
- 11. Kang HM, Subramaniam M, Targ S, Nguyen M, Maliskova L, McCarthy E. Multiplexed
  droplet single-cell RNA-sequencing using natural genetic variation. Nat Biotechnol. 2018;
  36(1):89-94.
- 12. Gehring J, Park JH, Chen S, Thomson M, Pachter L. Highly Multiplexed Single-Cell RNA seq for Defining Cell Population and Transcriptional Spaces. 2018. Preprint: bioRxiv doi:
  10.1101/315333.
- 13. Guo C, Biddy BA, Kamimoto K, Kong W, Morris SA. CellTag Indexing: a genetic barcode based multiplexing tool for single- cell technologies. 2018. Preprint: bioRxiv doi:
  10.1101/335547.
- 14. Rosenberg AB, Roco CM, Muscat RA, Kuchina A, Sample P, Yao Z, et al. Single-cell
  profiling of the developing mouse brain and spinal cord with split-pool barcoding. Science.
  2018; 360(6385):176-182.
- 15. Islam S, Zeisel A, Joost S, La Manno G, Zajac P, Kasper M, Lönnerberg P, Linnarsson
  S. Quantitative single-cell RNA-seq with unique molecular identifiers. Nat Methods. 2014;
  11(2):163-6.
- 16. Ziegenhain C, Vieth B, Parekh S, Reinius B, Guillaumet-Adkins A, Smets M, et al.
  Comparative Analysis of Single-Cell RNA Sequencing Methods. Mol Cell. 2017.
  65(4):631-643.e4.
- 17. Butler A, Hoffman P, Smibert P, Papalexi E, Satija R. Integrating single-cell transcriptomic
  data across different conditions, technologies, and species. Nat Biotechnol. 2018; doi:
  10.1038/nbt.4096.
- 18. van der Maaten L, Hinton G. Visualizing Data using t-SNE. J. Mach. Learn. Res. 2008; 9:
  2579–2605.
- 19. Sing T, Sander O, Beerenwinkel N, Lengauer T. ROCR: visualizing classifier performance
  in R. Bioinformatics. 2005; 21(20): 3940-1.
- 20. Robin X, Turck N, Hainard A, Tiberti N, Lisacek F, Sanchez JC, Müller M. pROC: an open source package for R and S+ to analyze and compare ROC curves. BMC Bioinformatics,
  2011; 12: 77.
- 314
- 315
- 316
- 317
- 318
- 319 320
- 321
- 322
- 323
- 324
- 325
- 326

327 328

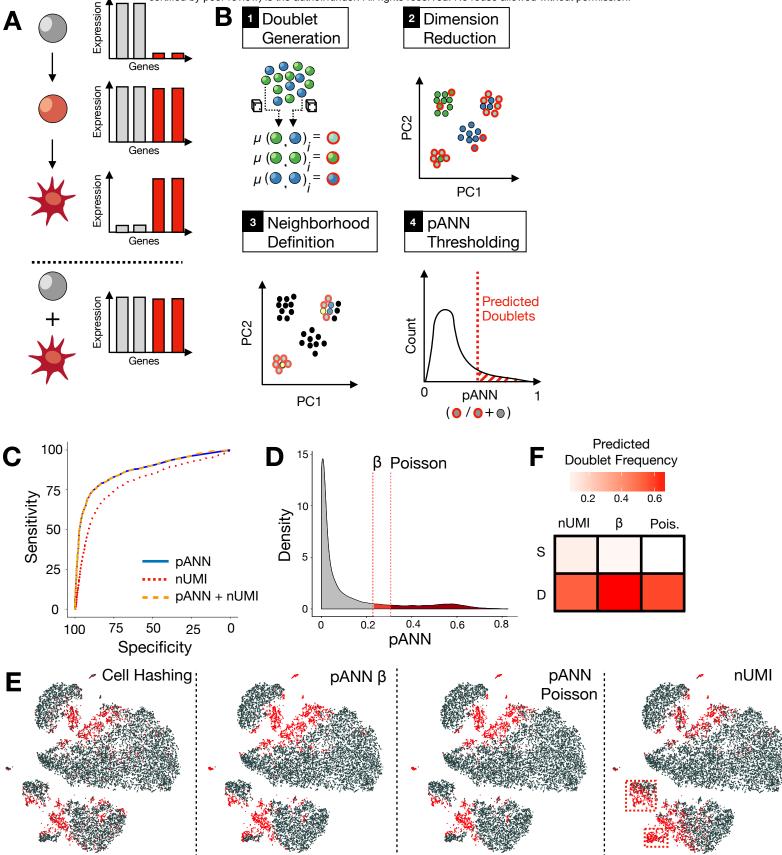
# 329330 FIGURE LEGENDS

331

332 Figure 1: DoubletFinder robustly predicts Cell Hashing doublets and outperforms nUMI thresholding. (A) Schematic describing importance of doublet detection. Developmental 333 intermediates (light red) can express genes associated with both progenitor (grey) and 334 335 differentiated (dark red) cell types. Doublets formed from progenitor and mature cells may mimic the expression profile of intermediate cell states, and thereby confound analysis. (B) Schematic 336 of DoubletFinder workflow. After artificial doublet (red outline) generation, the proportion of 337 338 artificial nearest neighbors is defined for every real cell (examples highlighted yellow). These 339 results are thresholded to define doublet predictions. (C) Density plot of pANN values with red 340 dotted lines denoting expected doublet thresholds. Histogram is colored according to whether the cells were called as singlets (grey) or doublets by one (light red) or both thresholding 341 strategies (dark red). (D) t-SNE visualization of real and predicted Cell Hashing doublets (red) 342 343 and singlets (grey), DoubletFinder predictions, and nUMI thresholding predictions. nUMI 344 predictions deviate significantly from Cell Hashing results (red dashed boxes). (E) Heat map showing the proportion of DoubletFinder and nUMI-predicted doublets present in Cell Hashing 345 346 singlet (S) and doublet (D) groups. (F) ROC analysis of logistic regression models trained using 347 nUMIs alone (dotted red), pANN alone (solid blue) and both nUMIs and pANN (dashed orange) 348 as features.

349 Figure 2: DoubletFinder detects false-negative and false-positive doublet predictions in Cell Hashing and Demuxlet datasets. (A) t-SNE visualization of real and predicted Cell 350 351 Hashing doublets (red) and singlets (grey) highlighting a doublet-enriched, 'speckled' region. (B) Violin plots describing the distribution of marker gene expression in high-confidence doublets 352 353 (red), putative false-negatives (blue), and singlet B-cells (teal) and NK cells (orange). (C) Barcode UMI box plots for the 1<sup>st</sup> and 2<sup>nd</sup> most abundant barcodes in high-confidence singlets 354 (black) and doublets (red), as well as false-negative singlets (blue). (D) t-SNE visualization of 355 356 real and predicted Demuxlet doublets (red) and singlets (grey) highlighting putative falsepositives. (E) Violin plots describing the contributions of homotypic and heterotypic doublets to 357 each DoubletFinder-defined doublet's nearest neighborhood. t-SNE visualization of putative 358 homotypic and heterotypic doublet clusters in gene expression space. (F) RNA UMI box plots 359 for high- confidence singlets (black) and doublets (red) as well as discordant doublet predictions 360 361 between Demuxlet and DoubletFinder (orange).

bioRxiv preprint doi: https://doi.org/10.1101/352484; this version posted July 19, 2018. The copyright holder for this preprint (which was not certified by peer review) is the author/funder. All rights reserved. No reuse allowed without permission.



bioRxiv preprint doi: https://doi.org/10.1101/352484; this version posted July 19, 2018. The copyright holder for this preprint (which was not certified by peer review) is the author/funder. All rights reserved. No reuse allowed without permission.

